Int. J. Heat Mass Transfer. Vol. 33, No. 8, pp. 1633–1641, 1990
Printed in Great Britain

0017-9310/90 $3.00 + 0.00


# Adaptive grid method for convection–diffusion equations

ADENIYI LAWAL
Department of Chemical Engineering, University of Port Harcourt, P.M.B. 5323, Port Harcourt, Nigeria

(*Received* 9 *March* 1989 *and in final form* 22 *September* 1989)

**Abstract**—Numerical solutions to the classical Graetz problem in the entrance region of a pipe produce estimates of the Nusselt number which are greatly in error except when the uniform grid is extremely fine, leading to huge storage requirements. The use of adaptive grids, it is proposed, will resolve the twin problem of excessive storage space and inaccuracy of results. Therefore, two adaptive grids using different methods of generating the weighting function are developed and tested in this work. One of the adaptive grids produced results that compared favourably with the exact solution with as few as 11 grid points. With the uniform grid, as many as 301 grid points would have been required.

## INTRODUCTION

TRANSPORT processes commonly encountered in industrial practice are modelled by equations with convective transport in a predominant flow direction (usually axial) and diffusive transport in a perpendicular direction. Another possible feature of such models is a discontinuity in boundary condition experienced by the fluid in entering the duct. If, for instance, the entry profiles are uniform and a step change occurs in the entrance, then boundary layers characterized by large gradients develop close to the walls of the duct. Consequently, close to the duct entrance (the region of interest) either for analytical or numerical purposes, all we have is a thin layer next to the walls, since the bulk of the fluid outside this layer has not felt the presence of the walls. This behaviour is not limited to the heat transfer problem as examples are legion even in mass transfer processes.

One such model problem is the hydrodynamically developed but thermally developing heat transfer to a Newtonian fluid in a circular duct governed by the classical Graetz equation. Despite its obvious simplicity, the Graetz problem has provided useful guidance in the design of heat exchangers. Of greater significance is the fact that it has served as a model problem for testing various solution techniques, since its solution has been well established [1]. The problem was first solved by Graetz in 1883 using the separation of variables technique. He evaluated the first two eigenvalues and eigenfunctions and since this historical attempt, other innumerable studies have sought to extend his work by providing more terms of the series solution. It is well known that even with 121 terms, the series solution does not converge near the duct entrance. A partial resolution of the difficulty was suggested by Leveque [2], who employed the 'flat plate' solution near the singularity at the entrance.

Numerical solution techniques using the finite-difference scheme have fared even worse. The extended Graetz problem, which included axial heat conduction, was solved numerically by Schmidt and Zeldin [3] using 41 grid points in each coordinate direction. Deviations of up to 25% were observed in the local Nusselt number close to the entrance. In Grigull and Tratz [4], mean Nusselt numbers were in error by as much as 16% when compared with the Leveque solutions. A numerical investigation by Conley *et al.* [5] revealed that all these efforts failed because of the inadequate resolution of the thermal gradients near the duct walls by the coarse grids employed. As many as 301 grid points were required to replicate the analytical solution. Such fine grids would place excessive demands on computer storage requirements if they were to be employed for problems of practical and industrial relevance, which often times are governed by complex transport equations.

A more economic method is evidently desirable. The occurrence of large gradients near the wall suggests that grids should be appropriately concentrated in this region, thus placing available computing power in an area where it is desired most. Since the extent of this region is not known a priori, the grid placement method to be adopted must possess an in-built mechanism for delimiting the region. In addition, since such problems are often times evolutionary in nature, usually spatially, grid point deployment must be altered in response to the changes in the numerical solution from one duct location to the next. The adaptive grid method, which is increasingly gaining attention in computational fluid dynamics research, seems to be an attractive option worth investigating.

The adaptive grid method dynamically concentrates grid points in regions of rapid variation of solution by equidistributing some weighting function of the solution. The weighting function is normally

## NOMENCLATURE

| | | | |
|---|---|---|---|
| $C_p$ | heat capacity | $w_i$ | weighting function at grid point $i$ |
| $k$ | thermal conductivity | $x$ | axial coordinate |
| $Nu_{X^*}$ | local Nusselt number | $X^*$ | axial coordinate, $(x/2r_0)/Pe$ [dimensionless] |
| $Pe$ | Peclet number, $2r_0\rho C_p u_m/k$ | $z$ | coordinate function, $(1-R_i)^3/9X^*$. |
| $r$ | radial coordinate | | |
| $r_0$ | tube radius | | |
| $R$ | radial coordinate, $r/r_0$ [dimensionless] | Greek symbols | |
| $R_i$ | radial coordinate at grid point $i$ | $\alpha$ | thermal diffusivity, $\rho C_p/k$ |
| $T$ | temperature | $\zeta$ | radial coordinate |
| $T_e$ | entrance temperature | $\eta$ | axial coordinate |
| $T_w$ | wall temperature | $\theta$ | temperature [dimensionless] |
| $u$ | velocity | $\theta_b$ | bulk temperature [dimensionless] |
| $u_m$ | mean velocity | $\rho$ | density. |

chosen to reflect the solution gradient and the varied forms of the weighting function, their weaknesses and merits can be found in Thompson *et al.* [6].

In the present study, the Graetz problem will be solved using three different grid types—two adaptive grids and the regular uniform grid. The first adaptive grid will be constructed from a solution known a priori and available analytically. The Leveque solution has been selected for this purpose and it needs to be mentioned that in the strictest sense, the grid thus obtained is not adaptive. The second adaptive grid is generated from the numerical solution to the Graetz problem and is thus truly adaptive. The three grid types will be compared in terms of accuracy of solution, storage and CPU time requirements.

## ANALYSIS

The problem to be investigated is the entrance region laminar heat transfer to viscous incompressible constant property Newtonian fluid flowing in a circular tube with a fully developed entrance velocity profile. The fluid enters the duct with a uniform temperature $T_e$ while the duct wall is maintained at $T_w$, which is different from the entrance value. Such effects as viscous dissipation, internal heat generation, axial heat conduction and natural convection are assumed to be negligible. With the foregoing assumptions, the thermal energy equation and the boundary conditions are

$$\frac{1}{r}\frac{\partial}{\partial r}\left(r\frac{\partial T}{\partial r}\right)=\frac{u}{\alpha}\frac{\partial T}{\partial x} \tag{1a}$$

$$T(r,0)=T_e;\quad T(r_0,x)=T_w \quad \text{and} \quad \frac{\partial T}{\partial r}(0,x)=0. \tag{1b}$$

To render the equations non-dimensional, we introduce the following variables and substitute for the parabolic velocity profile:

$$R=r/r_0$$

$$\theta=\frac{T-T_w}{T_e-T_w}$$

$$X^*=(x/2r_0)/Pe$$

to obtain

$$\frac{2}{R}\frac{\partial}{\partial R}\left(R\frac{\partial\theta}{\partial R}\right)=(1-R^2)\frac{\partial\theta}{\partial X^*} \tag{2a}$$

$$\theta(R,0)=1.0;\quad \theta(1,X^*)=0 \quad \text{and} \quad \frac{\partial\theta}{\partial R}(0,X^*)=0. \tag{2b}$$

Equation (2a) is parabolic with the axial coordinate serving as a time-like coordinate. Whereas the radial coordinate is delimited, the axial coordinate is unbounded and can therefore, in principle, span the infinite domain. Numerically, however, a limit needs to be imposed. Usually, computation is discontinued when changes in a gross property (e.g. $Nu_{X^*}$) become insignificant. Since the solution at the entrance is known (from the entrance condition) to initiate the numerical solution, an axial step is taken and the equation solved at that location. We proceed to the next location and the procedure is repeated. In view of all these and the fact that the boundary layer develops in the radial direction, grid adaption need only be effected radially. Cognizance must, however, be taken that the radial coordinate now becomes dependent on the axial coordinate and equation (2a) modified accordingly.

Since it is more convenient to solve equation (2a) with uniform spacing, let the $(R, X^*)$ coordinate be transformed to the $(\zeta, \eta)$ coordinate such that variable spacing in $(R, X^*)$ corresponds to uniform spacing in

$(\zeta, \eta)$. Hence

$$\left.\frac{\partial\theta}{\partial X^*}\right|_R = \left.\frac{\partial\theta}{\partial\zeta}\right|_\eta \frac{\mathrm{d}\zeta}{\mathrm{d}X^*} + \left.\frac{\partial\theta}{\partial\eta}\right|_\zeta \frac{\mathrm{d}\eta}{\mathrm{d}X^*} - \left.\frac{\partial\theta}{\partial R}\right|_{X^*} \frac{\mathrm{d}R}{\mathrm{d}X^*} \quad (3a)$$

$$\left.\frac{\partial\theta}{\partial R}\right|_{X^*} = \left.\frac{\partial\theta}{\partial\zeta}\right|_\eta \left(\frac{\partial\zeta}{\partial R}\right)_{X^*} + \left(\frac{\partial\theta}{\partial\eta}\right)_\zeta \left(\frac{\partial\eta}{\partial R}\right)_{X^*} \quad (3b)$$

and

$$\left.\frac{\partial^2\theta}{\partial R^2}\right|_{X^*} = \zeta_{RR}\left.\frac{\partial\theta}{\partial\zeta}\right|_\eta + \eta_{RR}\left.\frac{\partial\theta}{\partial\eta}\right|_\zeta + 2\zeta_R\eta_R\frac{\partial^2\theta}{\partial\zeta\,\partial\eta} + \zeta_R^2\left.\frac{\partial^2\theta}{\partial\zeta^2}\right|_\eta + \eta_R^2\left.\frac{\partial^2\theta}{\partial\eta^2}\right|_\zeta. \quad (3c)$$

Using the following relationships:

$$\zeta_R = \frac{1}{R_\zeta} \quad (4a)$$

$$\zeta_{RR} = \frac{-R_{\zeta\zeta}}{R_\zeta^3} \quad (4b)$$

$$\eta_R = \frac{1}{R_\eta} \quad (4c)$$

$$\eta_{RR} = \frac{-R_{\eta\eta}}{R_\eta^3} \quad (4d)$$

equations (2a) and (2b) become, after substitution and rearrangement

$$\left\{\frac{2}{RR_\zeta} - \frac{2R_{\zeta\zeta}}{R_\zeta^3} - (1-R^2)\frac{\mathrm{d}\zeta}{\mathrm{d}X^*} + \frac{(1-R^2)}{R_\zeta}\frac{\mathrm{d}R}{\mathrm{d}X^*}\right\}\left.\frac{\partial\theta}{\partial\zeta}\right|_\eta + \left\{\frac{2}{RR_\eta} - \frac{2R_{\eta\eta}}{R_\eta^3} - (1-R^2)\frac{\mathrm{d}\eta}{\mathrm{d}X^*} + \frac{(1-R^2)}{R_\eta}\frac{\mathrm{d}R}{\mathrm{d}X^*}\right\}\left.\frac{\partial\theta}{\partial\eta}\right|_\zeta + \frac{4}{R_\zeta R_\eta}\frac{\partial^2\theta}{\partial\zeta\,\partial\eta} + \frac{2}{R_\zeta^2}\frac{\partial^2\theta}{\partial\zeta^2} + \frac{2}{R_\eta^2}\frac{\partial^2\theta}{\partial\eta^2} = 0 \quad (5a)$$

$$\theta(\zeta, 0) = 1.0,\ \theta(\zeta(R=1), X^*) = 0;\ \frac{\partial\theta}{\partial\zeta}(1, X^*) = 0. \quad (5b)$$

Equation (5a) is the Graetz problem written in generalized coordinates, but in this study, interest is restricted to the case

$$\eta = \eta(R, X^*) = \eta(X^*) = X^* \quad (6a)$$

$$\zeta = \zeta(R, X^*) = \zeta(R) \quad (6b)$$

whence equation (5a) becomes

$$\left\{\frac{2}{RR_\zeta} - \frac{2R_{\zeta\zeta}}{R_\zeta^3} + \frac{(1-R^2)}{R_\zeta}\frac{\mathrm{d}R}{\mathrm{d}X^*}\right\}\left(\frac{\partial\theta}{\partial\zeta}\right)_{X^*} + \frac{2}{R_\zeta^2}\frac{\partial^2\theta}{\partial\zeta^2} = (1-R^2)\left(\frac{\partial\theta}{\partial X^*}\right)_\zeta. \quad (7)$$

*Grid adaption*

The essence of most adaptive grid methods is the equidistribution, over a field, of some weighting function $w(R)$ and, for a one-dimensional problem, this can be stated mathematically as

$$\int_{R_i}^{R_{i+1}} w(R)\,\mathrm{d}R = \text{constant} \quad (8a)$$

or

$$\Delta R_i w_i = \text{constant} \quad (8b)$$

where $\Delta R_i$ is the grid interval and subscript $i$ denotes the grid point number. From equations (8a) and (8b), it is obvious that if the solution gradient is chosen as the weighting function, then wherever it assumes a large value, the grid interval will be small and vice versa. By construction, the $\zeta$ coordinate can be made to take on integral values such that $\Delta\zeta = 1$ and the maximum value of $\zeta$, i.e. $M$, is equal to the total number of points. Consequently

$$\Delta R = R_\zeta \Delta_\zeta = R_\zeta \quad (9)$$

so that equation (8b) becomes

$$R_\zeta w = \text{constant} = C. \quad (10a)$$

To evaluate the constant, we rewrite equation (10a) as

$$\zeta_R = \frac{w}{C} \quad (10b)$$

and integrate to obtain

$$M - 1 = \frac{1}{C}\int_0^1 w\,\mathrm{d}R \quad (11a)$$

or

$$C = \frac{1}{M-1}\int_0^1 w\,\mathrm{d}R. \quad (11b)$$

The general equation for the grid locations $R_i$ then follows:

$$\int_0^{R_i} \zeta_R\,\mathrm{d}R = \frac{1}{C}\int_0^{R_i} w\,\mathrm{d}R \quad (12a)$$

or

$$\frac{i-1}{M-1}\int_0^1 w(R)\,\mathrm{d}R = \int_0^{R_i} w(R)\,\mathrm{d}R \quad (i = 2, 3, \ldots, M-1). \quad (12b)$$

The coordinate transformation equation (12b) is in general coupled with equation (7a) rendered in discrete form and both equations have to be satisfied before proceeding to the next axial location.

*Choice of weighting function*

*Case a: uniform grid.* When the weighting function is set to 1, we recover the uniform grid.

*Case b: adaptive (Leveque) grid.* Here the weighting function $w(R)$ is chosen to be the thermal gradient $\partial\theta/\partial R$ with $\theta$ given by the Leveque solution, i.e.

$$\theta = \frac{1}{\Gamma(4/3)}\int_0^\xi \mathrm{e}^{-\sigma^3}\,\mathrm{d}\sigma \quad (13)$$

where $\xi = (1-R)/(9X^*)^{1/3}$. Equation (12b) then becomes

$$\int_0^{R_i} e^{-\xi^3}\,dR = \frac{i-1}{M-1}\int_0^1 e^{-\xi^3}\,dR. \quad (14)$$

To evaluate the integrals, we first make a change of variable from $R$ to $\xi$, and subsequently set $\xi^3 = y$ to obtain

$$-\frac{1}{3}\left[\int_0^{(1-R_i)^3/9X^*} y^{-2/3}e^{-y}\,dy - \int_0^{1/9X^*} y^{-2/3}e^{-y}\,dy\right] = \frac{i-1}{3(M-1)}\int_0^{1/9X^*} y^{-2/3}e^{-y}\,dy \quad (15a)$$

or

$$Q(\tfrac{1}{3},(1-R_i)^3/9X) = \Gamma(\tfrac{1}{3}) - \frac{M-i}{M-1}(\Gamma(\tfrac{1}{3}) - Q(\tfrac{1}{3},1/9X^*)) \quad (i=2,3,\ldots,M-1) \quad (15b)$$

where the $Q(a,z)$ function is given by

$$Q(a,z) = \int_z^\infty e^{-y}y^{a-1}\,dy. \quad (16)$$

For $0 \leqslant X^* \leqslant 10^4$ which is the range of interest, $Q(\frac{1}{3},1/9X^*) \ll \Gamma(\frac{1}{3})$; hence equation (15b) can be rewritten as

$$Q(\tfrac{1}{3},(1-R_i)^3/9X^*) = \Gamma(\tfrac{1}{3}) - \frac{(M-i)}{(M-1)}\Gamma(\tfrac{1}{3}) \quad (17a)$$

or

$$\gamma(\tfrac{1}{3},(1-R_i)^3/9X^*) = \frac{(M-i)}{M-1}\Gamma(\tfrac{1}{3}) \quad (i=2,3,\ldots,M-1) \quad (17b)$$

where

$$\gamma(a,z) = \int_0^z e^{-y}y^{a-1}\,dy = \Gamma(a) - Q(a,z).$$

Equation (17b) is a non-linear equation in $z$ or $(R_i)$ and substituting for the $\gamma(a,z)$ function, it becomes

$$\sum_{k=0}^{\infty}\frac{(-1)^k z^{(1/3)+k}}{k!(\frac{1}{3}+k)} = 2.678939\frac{(M-i)}{M-1} \quad (i=2,3,\ldots,M-1). \quad (18)$$

If we employ the Newton–Raphson method, the iteration equation at the $n+1$ level will be given by

$$z_{(n+1)} = z_{(n)} - \frac{\left[\sum_{k=0}^{\infty}\frac{(-1)^k z_{(n)}^{(1/3)+k}}{k!(\frac{1}{3}+k)} - 2.678939\frac{(M-i)}{M-1}\right]}{\sum_{k=0}^{\infty}\frac{(-1)^k z_{(n)}^{k-(2/3)}}{k!}} \quad (i=2,3,\ldots,M-1). \quad (19)$$

*Case c: conventional adaptive grid.* The weighting function is chosen to be

$$w = 1+\beta|\partial\theta/\partial R|/|\partial\theta/\partial R|_{\max} \quad (20)$$

where $\beta$ is a constant taken as 1.0 in this work.

*Method of solution*

A standard grid network with the dependent variable stored at each grid point is laid out on the computational domain having a uniform radial spacing of $\Delta\zeta$ but variable spacing in $R$. In equation (7a), a second-order central difference scheme is employed in approximating all partial derivatives in the radial direction and the upwind scheme for the first-order derivative in the axial direction. The scale factors $R_{,\zeta}$, $R_{,\zeta\zeta}$ and the variable radial spacing $R$ are evaluated from the coordinate transformation equations. For the uniform grid, the results are straightforward and there is no coupling between the energy equation and the coordinate transformation equation. However, this is not true for the two adaptive grids. In the case of the adaptive (Leveque) grid, equation (19) is solved iteratively for $z$ until there is convergence. Here, the convergence criterion defined as change in variable during the iteration divided by the previous value was set to $10^{-5}$. Twenty-one terms were found to be sufficient for accuracy in the series for the range of $X^*$ considered. With the $z(R_i)$ values, the discretized form of equation (7a) can then be solved and we proceed to the next axial location.

With the conventional adaptive grid (case c), both the energy equation and the coordinate transformation equation need be solved simultaneously since the weighting function depends on $\theta$, which is not known a priori unlike in the case of the adaptive (Leveque) grid. The implementation of the method is initiated on a uniform grid which provides rough estimates for the thermal gradients across the radial domain. The location where there is a large change in thermal gradient is assumed to define the boundary layer. This region is next subdivided uniformly and the energy equation solved. With the thermal gradients at these new grid locations, the coordinate transformation equation can now be solved for the $R_i$s. Associated with these $R_i$s are new values of temperature $\theta$; therefore there is need for iteration which is discontinued when the $R_i$s do not change appreciably. At this point, we can proceed to the next axial location and the procedure can be repeated.

Upon obtaining the temperature profile, we calculate two quantities of special interest, the dimensionless bulk temperature $\theta_b$, and the local Nusselt number $Nu_{X^*}$. To evaluate $\theta_b$, the energy equation is integrated over a control volume of thickness $\Delta X^*$ to give

$$\theta_b(X^*) = \theta_b(X^*-\Delta X^*) + 4X^*\left[\frac{\partial\theta}{\partial R}\bigg|_{R=1}^{(X^*)} - \frac{\partial\theta}{\partial R}\bigg|_{R=1}^{(X^*-\Delta X^*)}\right] \quad (21a)$$

while $Nu_{X^*}$ is obtained from

$$Nu_{X^*} = \frac{-2\left.\frac{\partial\theta}{\partial R}\right|_{R=1}}{\theta_b}. \quad (21b)$$

For the purpose of comparison, the thermal gradient in equations (21a) and (21b) was evaluated numerically using the 2-point, 3-point and 5-point rules. The $\theta_b$ and $Nu_{X^*}$ values so obtained have been designated accordingly.

## RESULTS AND DISCUSSION

The values of $\theta_b$ and $Nu_{X^*}$ as obtained from the different grids considered in this study are presented in Tables 1–9. The computation in each case was initiated with an axial step size $\Delta X^*$ of $10^{-7}$ and for each order of magnitude change in $X^*$, a corresponding change in $\Delta X^*$ was made. The results of Shah and London [1], also included in the tables, were obtained from analytical solution of Leveque's problem.

In Tables 1–3, the size of the uniform grid is varied to determine the optimum size for accurate values of the gross properties $\theta_b$ and $Nu_{X^*}$. The size so obtained is then used to assess the storage and CPU time requirements for the adaptive grids. With $M = 21$, the $\theta_b$ and $Nu_{X^*}$ values are greatly in error even at $X^* = 10^{-4}$, an axial coordinate sufficiently far from the entrance. In addition, the value of $Nu_{X^*}$ is dependent on the expression employed in approximating the thermal gradient; the arbitrariness so introduced further attests to the unsuitability of this grid size. When the number of radial grid points is increased to 101, the results are still unacceptable, even though a noticeable improvement in the accuracy of the results is obtained. Further refinement of the grid ($M = 301$) produces results which can be considered accurate enough for the purpose of comparison. Therefore, this grid size is appropriately assigned a factor of

Table 1. $\theta_b$ and $Nu_{X^*}$ from the uniform grid at $X^* = 10^{-6}$

| | Number of grid points | | | |
|---|---|---|---|---|
| | 21 | 101 | 301 | Shah and London [1] |
| $\theta_b^{(2)}$ | 0.9998 | 0.9994 | 0.9993 | 0.9994 |
| $\theta_b^{(3)}$ | 0.9998 | 0.9992 | 0.9993 | 0.9994 |
| $\theta_b^{(5)}$ | 0.9997 | 0.9991 | 0.9993 | 0.9994 |
| $Nu_{X^*}^{(2)}$ | 39.6725 | 110.0190 | 109.2110 | 106.5380 |
| $Nu_{X^*}^{(3)}$ | 59.3469 | 130.5790 | 109.8190 | 106.5380 |
| $Nu_{X^*}^{(5)}$ | 82.0273 | 116.3660 | 108.7670 | 106.5380 |
| Storage factor | 0.684 | 0.774 | 1.0 | — |
| CPU time factor | 0.208 | 0.457 | 1.0 | — |

Table 2. $\theta_b$ and $Nu_{X^*}$ from the uniform grid at $X^* = 10^{-5}$

| | Number of grid points | | | |
|---|---|---|---|---|
| | 21 | 101 | 301 | Shah and London [1] |
| $\theta_b^{(2)}$ | 0.9985 | 0.9970 | 0.9969 | 0.9971 |
| $\theta_b^{(3)}$ | 0.9977 | 0.9967 | 0.9969 | 0.9971 |
| $\theta_b^{(5)}$ | 0.9969 | 0.9968 | 0.9969 | 0.9971 |
| $Nu_{X^*}^{(2)}$ | 36.9692 | 50.1998 | 50.0394 | 48.9140 |
| $Nu_{X^*}^{(3)}$ | 53.9836 | 50.9346 | 49.9938 | 48.9140 |
| $Nu_{X^*}^{(5)}$ | 71.4184 | 49.2084 | 49.9557 | 48.9140 |
| Storage factor | 0.684 | 0.774 | 1.0 | — |
| CPU time factor | 0.198 | 0.451 | 1.0 | — |

Table 3. $\theta_b$ and $Nu_{X^*}$ from the uniform grid at $X^* = 10^{-4}$

| | Number of grid points | | | |
|---|---|---|---|---|
| | 21 | 101 | 301 | Shah and London [1] |
| $\theta_b^{(2)}$ | 0.9881 | 0.9860 | 0.9860 | 0.9866 |
| $\theta_b^{(3)}$ | 0.9840 | 0.9857 | 0.9860 | 0.9866 |
| $\theta_b^{(5)}$ | 0.9815 | 0.9859 | 0.9860 | 0.9866 |
| $Nu_{X^*}^{(2)}$ | 23.4032 | 22.8911 | 22.8155 | 22.2750 |
| $Nu_{X^*}^{(3)}$ | 28.4465 | 22.8288 | 22.7797 | 22.2750 |
| $Nu_{X^*}^{(5)}$ | 26.2373 | 22.7749 | 22.7775 | 22.2750 |
| Storage factor | 0.684 | 0.774 | 1.0 | — |
| CPU time factor | 0.194 | 0.449 | 1.0 | — |

unity for storage and CPU time requirements. The percentage error in $Nu_{X^*}$ from $X^* = 10^{-6}$ to $10^{-4}$ averages about 2.4% and is never greater than 3% with Shah and London's results used as bases.

In Tables 4–6, the results from the adaptive (Leveque) grid (ALG) and adaptive grid (AG), both with 11 nodal points, and the uniform grid ($M = 301$) are presented. At $X^* = 10^{-6}$, the two adaptive grids produced the same values of $\theta_b$ which are not different from that obtained by Shah and London; however, the $Nu_{X^*}$ from the ALG is in error by about 12.5%, the AG by less than 1.5% and the uniform grid by 3%. It is noteworthy that the storage and CPU time requirements for the adaptive grids are significantly less than those for the uniform grid. As $X^*$ increases, there is a marginal decrease in the CPU time requirements but the error in $Nu_{X^*}$ still remains substantially high for the ALG (13% at $X^* = 10^{-5}$ and 14% at $X^* = 10^{-4}$) and low ($\sim 1.5\%$) for the AG, with the AG consistently performing better than the uniform grid. The axial variation of $Nu_{X^*}$ for the different grids is indicated in Fig. 1 while sample radial profiles of temperature are as shown in Figs. 2(a) and (b).

When the number of adaptive grid points is increased to 21, the results of Tables 7–9 indicate some slight improvement in the accuracy of the ALG

Table 4. $\theta_b$ and $Nu_{X^*}$ from the adaptive grids at $X^* = 10^{-6}$

| | Adaptive (Leveque) grid | Adaptive grid | Uniform grid | |
|---|---|---|---|---|
| | Number of grid points | | | |
| | 11 | 11 | 301 | Shah and London [1] |
| $\theta_b^{(2)}$ | 0.9993 | 0.9993 | 0.9993 | 0.9994 |
| $\theta_b^{(3)}$ | 0.9993 | 0.9993 | 0.9993 | 0.9994 |
| $\theta_b^{(5)}$ | 0.9993 | 0.9993 | 0.9993 | 0.9994 |
| $Nu_{X^*}^{(2)}$ | 119.9830 | 107.6120 | 109.2110 | 106.5380 |
| $Nu_{X^*}^{(3)}$ | 120.0110 | 108.0150 | 109.8190 | 106.5380 |
| $Nu_{X^*}^{(5)}$ | 119.8900 | 107.6130 | 109.7670 | 106.5380 |
| Storage factor | 0.726 | 0.771 | 1.0 | — |
| CPU time factor | 0.762 | 0.826 | 1.0 | — |

Table 5. $\theta_b$ and $Nu_{X^*}$ from the adaptive grids at $X^* = 10^{-5}$

| | Adaptive (Leveque) grid | Adaptive grid | Uniform grid | |
|---|---|---|---|---|
| | Number of grid points | | | |
| | 11 | 11 | 301 | Shah and London [1] |
| $\theta_b^{(2)}$ | 0.9966 | 0.9970 | 0.9969 | 0.9971 |
| $\theta_b^{(3)}$ | 0.9966 | 0.9969 | 0.9969 | 0.9971 |
| $\theta_b^{(5)}$ | 0.9966 | 0.9970 | 0.9969 | 0.9971 |
| $Nu_{X^*}^{(2)}$ | 55.2732 | 49.6474 | 50.0394 | 48.9140 |
| $Nu_{X^*}^{(3)}$ | 55.2263 | 49.7108 | 49.9938 | 48.9140 |
| $Nu_{X^*}^{(5)}$ | 55.1709 | 49.4996 | 49.9557 | 48.9140 |
| Storage factor | 0.726 | 0.771 | 1.0 | — |
| CPU time factor | 0.754 | 0.821 | 1.0 | — |

Table 6. $\theta_b$ and $Nu_{X^*}$ from the adaptive grids at $X^* = 10^{-4}$

| | Adaptive (Leveque) grid | Adaptive grid | Uniform grid | |
|---|---|---|---|---|
| | Number of grid points | | | |
| | 11 | 11 | 301 | Shah and London [1] |
| $\theta_b^{(2)}$ | 0.9846 | 0.9863 | 0.9860 | 0.9866 |
| $\theta_b^{(3)}$ | 0.9846 | 0.9863 | 0.9860 | 0.9866 |
| $\theta_b^{(5)}$ | 0.9846 | 0.9864 | 0.9860 | 0.9866 |
| $Nu_{X^*}^{(2)}$ | 25.5037 | 22.0526 | 22.8155 | 22.2750 |
| $Nu_{X^*}^{(3)}$ | 25.4215 | 21.9997 | 22.7797 | 22.2750 |
| $Nu_{X^*}^{(5)}$ | 25.3955 | 21.8975 | 22.7775 | 22.2750 |
| Storage factor | 0.726 | 0.771 | 1.0 | — |
| CPU time factor | 0.753 | 0.820 | 1.0 | — |

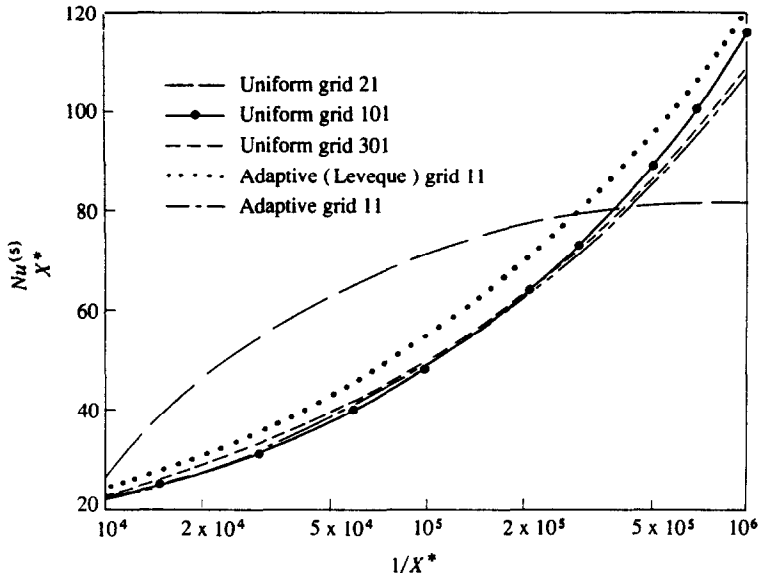


FIG. 1. Axial distribution of $Nu_{X^*}$ for the different grids.

results, with $Nu_{X^*}$ being in error by about 8%, a value which can still be considered unacceptably high. While the storage requirements continue to be far less than those for the fine uniform grid, significantly more CPU time is now required, especially for the AG. Based on the above results, the conventional adaptive grid is recommended. The results of the present exercise clearly indicate the gains that can be realized from the judicious use of grid points through adaptive gridding. While the storage requirements have been drastically reduced through the use of fewer grid points, the accuracy of the numerical results has not suffered, in fact a considerable improvement has been recorded for this one-dimensional problem.

If the results are extended to two dimensions, the storage reduction will be approaching about 50%, a value which is quite substantial. There is, as expected, an optimum number of grid points beyond which no noticeable improvement in the results is achieved. For the problem under consideration, 11 grid points seem to suffice if the conventional method of generating adaptive grids is adopted. Associated with this opti-

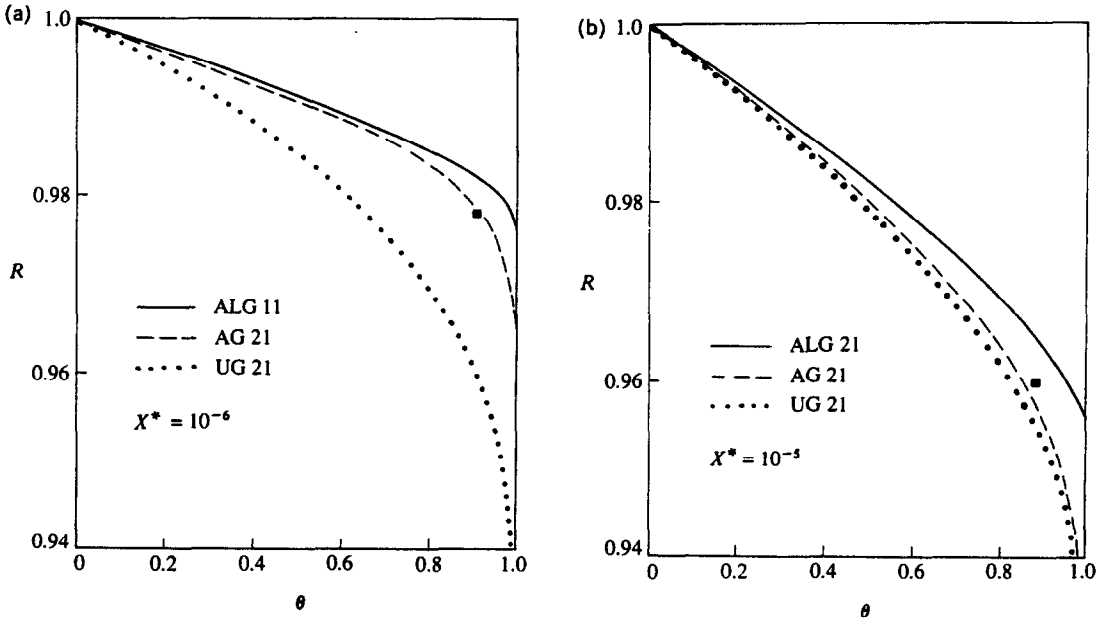


FIG. 2. (a) Radial temperature profiles for the different grids at $X^* = 10^{-6}$. (b) Radial temperature profiles for the different grids at $X^* = 10^{-5}$.

Table 7. $\theta_b$ and $Nu_{X^*}$ from the adaptive grids at $X^* = 10^{-6}$

| | Adaptive (Leveque) grid | Adaptive grid | Uniform grid | |
|---|---|---|---|---|
| | Number of grid points | | | |
| | 21 | 21 | 301 | Shah and London [1] |
| $\theta_b^{(2)}$ | 0.9993 | 0.9993 | 0.9993 | 0.9994 |
| $\theta_b^{(3)}$ | 0.9993 | 0.9993 | 0.9993 | 0.9994 |
| $\theta_b^{(5)}$ | 0.9993 | 0.9993 | 0.9993 | 0.9994 |
| $Nu_{X^*}^{(2)}$ | 114.6150 | 109.636 | 109.2110 | 106.5380 |
| $Nu_{X^*}^{(3)}$ | 114.5790 | 109.622 | 109.8190 | 106.5380 |
| $Nu_{X^*}^{(5)}$ | 114.5620 | 109.569 | 109.7670 | 106.5380 |
| Storage factor | 0.739 | 0.784 | 1.0 | — |
| CPU time factor | 1.474 | 2.005 | 1.0 | — |

Table 8. $\theta_b$ and $Nu_{X^*}$ from the adaptive grids at $X^* = 10^{-5}$

| | Adaptive (Leveque) grid | Adaptive grid | Uniform grid | |
|---|---|---|---|---|
| | Number of grid points | | | |
| | 21 | 21 | 301 | Shah and London [1] |
| $\theta_b^{(2)}$ | 0.9968 | 0.9969 | 0.9969 | 0.9971 |
| $\theta_b^{(3)}$ | 0.9968 | 0.9969 | 0.9969 | 0.9971 |
| $\theta_b^{(5)}$ | 0.9968 | 0.9969 | 0.9969 | 0.9971 |
| $Nu_{X^*}^{(2)}$ | 52.5613 | 50.2486 | 50.0394 | 48.914 |
| $Nu_{X^*}^{(3)}$ | 52.5162 | 50.1956 | 49.9938 | 48.914 |
| $Nu_{X^*}^{(5)}$ | 52.5086 | 50.1822 | 49.9557 | 48.914 |
| Storage factor | 0.739 | 0.784 | 1.0 | — |
| CPU time factor | 1.470 | 2.138 | 1.0 | — |

Table 9. $\theta_b$ and $Nu_{X^*}$ from the adaptive grids at $X^* = 10^{-4}$

| | Adaptive (Leveque) grid | Adaptive grid | Uniform grid | |
|---|---|---|---|---|
| | Number of grid points | | | |
| | 21 | 21 | 301 | Shah and London [1] |
| $\theta_b^{(2)}$ | 0.9853 | 0.9860 | 0.9860 | 0.9866 |
| $\theta_b^{(3)}$ | 0.9854 | 0.9860 | 0.9860 | 0.9866 |
| $\theta_b^{(5)}$ | 0.9854 | 0.9860 | 0.9860 | 0.9866 |
| $Nu_{X^*}^{(2)}$ | 24.1119 | 22.9514 | 22.8155 | 22.2750 |
| $Nu_{X^*}^{(3)}$ | 24.0627 | 22.8926 | 22.7797 | 22.2750 |
| $Nu_{X^*}^{(5)}$ | 24.0594 | 22.8773 | 22.7775 | 22.2750 |
| Storage factor | 0.739 | 0.784 | 1.0 | — |
| CPU time factor | 1.473 | 2.181 | 1.0 | — |

mum is a CPU time considerably less than that for a uniform grid of the same accuracy. Above this optimum value, the CPU time increases considerably. However, the most important consideration is not the CPU time but the storage requirement, as happens when for example a micro-computer with limited storage space is all that is available to the user.

## CONCLUSIONS

An adaptive grid with the weighting function generated through the conventional method has been successfully developed. With as few as 11 grid points, numerical results having better accuracy than a uniform grid of 301 grid points have been obtained. Consequently, storage requirements have been reduced and an extension to two- or three-dimensional problems, which is straightforward, will result in even greater reduction. While the CPU time requirement is usually not an important consideration when the situation calls for fewer grid points, it has been observed that this factor is not increased by adaptive grids unless the optimum number of grid points is exceeded.

*Acknowledgements*—The author wishes to express his gratitude to the University of Port Harcourt Computing Centre for providing the computing time required for this work. The typing of the manuscript was excellently done Mr D. O. Chuku.

## REFERENCES

1. R. K. Shah and A. L. London, Laminar forced convection in ducts. In *Advances in Heat Transfer*. Academic Press, New York (1978).
2. M. A. Leveque, Les lois de la transmission de chaleur par convection, *Ann. Mines Mem., Ser. 12* **13**, 201–299, 305–362, 381–415 (1928).
3. F. W. Schmidt and B. Zeldin, Laminar heat transfer in the entrance region of ducts, *Appl. Scient. Res.* **23**, 73–94 (1970).
4. U. Grigull and H. Tratz, Thermischer einlauf in ausgebildeter laminarer Rohrstromung, *Int. J. Heat Mass Transfer* **8**, 669–678 (1965).
5. N. Conley, A. Lawal and A. S. Mujumdar, An assessment of the accuracy of numerical solutions to the Graetz problem, *Int. Commun. Heat Mass Transfer* **12**, 209–218 (1985).
6. J. F. Thompson, Z. U. A. Warsi and C. W. Mastin, *Numerical Grid Generation* (1st Edn), pp. 378–387. Elsevier, New York (1985).

## METHODE DE GRILLE ADAPTATIVE POUR LES EQUATIONS DE CONVECTION ET DIFFUSION

**Résumé**—Les solutions numériques du problème classique de Graetz dans la région d'entrée d'un tuyau donnent des estimations du nombre de Nusselt qui sont très erronées sauf quand la grille uniforme est extrêmement fine, ce qui conduit à des besoins énormes de mémoire. Alors est proposée l'utilisation des grilles adaptatives pour résoudre à la fois les problèmes liés de la mémoire excessive et de l'imprécision des résultats. Par suite, dans ce travail sont développées et testées deux grilles adaptatives utilisant des méthodes différentes de génération des fonctions de pondération. L'une des grilles donne des résultats qui s'accordent bien avec la solution exacte avec seulement 11 points. Avec la grille uniforme, il faut 301 points pour atteindre la même résultat.

## EIN VERFAHREN MIT ANGEPASSTEM GITTER FÜR KONVEKTIONS-DIFFUSIONS-GLEICHUNGEN

**Zusammenfassung**—Numerische Lösungen für das klassische Graetz-Problem im Eingangsbereich eines Rohres führen zu Abschätzungen für die Nusselt-Zahl, die mit einem großen Fehler versehen sind. Dies kann bei Wahl eines gleichmäßigen, extrem feinen Gitters vermieden werden, was jedoch zu einem riesigen Speicherbedarf führt. Die vorgeschlagene Verwendung eines angepaßten Gitters löst das Doppelproblem eines riesenhaften Speicherbedarfs und einer Ungenauigkeit der Ergebnisse. Daher werden zwei angepaßte Gitter entwickelt und getestet, die unterschiedliche Verfahren bei der Generierung der Gewichtungsfunktion verwenden. Eines der angepaßten Gitter liefert Ergebnisse, die bei Verwendung von nur 11 Gitterpunkten recht gut mit der exakten Lösung übereinstimmen. Bei Wahl eines gleichmäßigen Gitters hätte man 301 Gitterpunkte benötigt.

## МЕТОД АДАПТИВНЫХ СЕТОК ДЛЯ УРАВНЕНИЙ КОНВЕКЦИИ И ДИФФУЗИИ

**Аннотация**—Численные решения классической задачи Гретца для входного участка трубы позволяют получить оценки числа Нуссельта, которые имеют погрешности во всех случаях, за исключением мелкоячеистой сетки постоянного размера, что вызывает необходимость большого объема памяти. Предполагается, что использование адаптивных сеток разрешит проблему большого объема памяти и неточности результатов. С этой целью на основе различных методов образования весовой функции разработаны и проверены две адаптивные сетки. Результаты, полученные с использованием одной из них, удовлетворительно согласуются с точным решением для 11 точек сетки. Для сетки постоянного размера необходимы 301 точек.